3D In Vitro Neuron on a Chip for Probing Calcium Mechanostimulation

Justin Bobo,* Akash Garg, Prahatha Venkatraman, Manoj Puthenveedu, and Philip R. LeDuc*

The evolution of tissue on a chip systems holds promise for mimicking the response of biological functionality of physiological systems. One important direction for tissue on a chip approaches are neuron-based systems that could mimic neurological responses and lessen the need for in vivo experimentation. For neural research, more attention has been devoted recently to understanding mechanics due to issues in areas such as traumatic brain injury (TBI) and pain, among others. To begin to address these areas, a 3D Nerve Integrated Tissue on a Chip (NITC) approach combined with a Mechanical Excitation Testbed (MET) System is developed to impose external mechanical stimulation toward more realistic physiological environments. PC12 cells differentiated with nerve growth factor, which were cultured in a controlled 3D scaffolds, are used. The cells are labeled in a 3D NITC system with Fluo-4-AM to examine their calcium response under mechanical stimulation synchronized with image capture. Understanding the neural responses to mechanical stimulation beyond 2D systems is very important for neurological studies and future personalized strategies. This work will have implications in a diversity of areas including tissue-on-a-chip systems, biomaterials, and neuromechanics.

1. Introduction

3D tissue-on-a-chip systems are considered promising candidates for a variety of fields including tissue engineering, organ regeneration, and in vitro disease models.[1–4] These multidimensional systems at a miniaturized scale seek to mimic physiology without using animals or humans. In these systems, 3D cell-to-cell interactions form potentially providing new in vitro approaches to study and mimic the response of biological and cellular processes. One particularly interesting area to study is mechanical stimulation due to its importance in a wide range of physiological systems from cardiac to neural areas. In the neural domain, previous approaches for examining the effects of in vitro mechanical loading on cells have focused mostly on local stimulation of single or multiple neurons cultured on planar substrates. These approaches have proven to be useful for understanding how mechanical stimuli are transduced to biochemical signals including being integrated with micro-fabricated environments.[5–8] While much of the knowledge of cellular biomechanics focuses on our understanding from planar substrates, these 2D systems unfortunately lack physiological aspects such as three dimensionality as well as the complexity of tissue and neuronal function. 3D culture systems can enhance the analysis of integrated interactions between tissue and neural response to recapitulate the natural microenvironment with spatiotemporal details, which may be relevant in understanding many issues including Alzheimer's disease and traumatic brain injury (TBI).[9,10,11]

This type of understanding of biomechanics is particularly important as TBI can result from a diversity of situations such as a car crash, an innocuous fall, sports injury, and sudden jolts or blows to the head. Annually these types of issues affect ≈1.5 million people in the United States and 69 million individuals worldwide as well as accounting for one third of all injury-related deaths in the United States affecting every stage of life from adolescents to the elderly.[12,13] Precisely identifying the importance of dysfunction and pathomorphological expressions after external mechanical insult is very important. These responses include a variety of factors such as compressive strains and subcellular responses. The approaches with tissue-on-a-chip systems could help in these areas as representative building blocks for assessing in vitro, multi-dimensional organ architectures toward physiological understanding and treatment.

Understanding cell responses under mechanical stimulation can be probed through many techniques. One approach involves an important molecular signature related

J. Bobo, A. Garg, Prof. P. R. LeDuc
Department of Mechanical Engineering
Carnegie Mellon University
5000 Forbes Ave, Pittsburgh, PA 15213, USA
E-mail: jbobo@andrew.cmu.edu; prl@andrew.cmu.edu
Dr. P. Venkatraman, Prof. M. Puthenveedu
Department of Pharmacology
University of Michigan
1150 W Medical Center Dr, Ann Arbor, MI 48109, USA
Prof. P. R. LeDuc
Department of Biological Sciences
Carnegie Mellon University
5000 Forbes Ave, Pittsburgh, PA 15213, USA

to mechanostimulation of calcium (Ca^{2+}) signaling. Ca^{2+} is an ubiquitous second messenger participating in signal transduction in cells throughout the body and is known to have roles in vital processes such as fertilization, muscle contraction, growth and development, neural transmission, and gene expression.[14–16] Ca^{2+} also plays a key role in the release of synaptic vesicles when a neuron fires, but this could lead to damage and cell death under an overload of the mitochondria and intense activation of Ca^{2+} dependent enzymes. Altered Ca^{2+} ion homeostasis is also linked to several neurodegenerative diseases: Parkinson's, Huntington's, Alzheimer's, amyotrophic lateral sclerosis, and TBI.[17–21] Although previous 2D studies of Ca^{2+} conducted in vitro examined Ca^{2+} concentrations related to stretch,[22] a complete understanding of neuronal functionality in a 3D platform combined with spatiotemporal detail, would provide tremendous insight to neuromechanical responses and potential treatments in the future.

Here, we developed a 3D collagen nerve integrated tissue on chip (NITC) system to mimic tissue engineering physiology. We then imposed mechanical stimulation on the NITC and examined Ca^{2+} responses under dynamic loading. Given the importance of compressive deformation to neurotrauma and impact injuries with understanding their long term effects, we believe that our approach will provide new knowledge in areas including neuromechanics, biomaterials, and 3D cellular response.

2. Results and Discussion

2.1. 3D Cellular Collagen Scaffolds under Mechanical Stimulation

To study Ca^{2+} response in nerve growth factor (NGF) induced PC12 cells, Fluo-4-AM (stock: 50 µg, molecular weight: 1097 g mol^{-1}), which is a cell permeant Ca^{2+} indicator, was introduced to the cells. Fluo-4-AM was pipetted onto the NGF induced PC12 cells, which were then incubated for 1 h.[23,24] Ca^{2+} stained cells were added to 10X phosphate buffered saline (PBS), sodium hydroxide (NaOH), and type 1 collagen to form a cross-linked ECM. Collagen type I, which is the most abundant protein found in mammals as well as being naturally present in many 3D matrices in various tissues, was used as the ECM.[25,26] The collagen concentration with embedded PC12 cells was 5 mg mL^{-1}, which allowed us to maintain structural stability while applying external mechanical, compressive loading. This concentration is slightly higher than in vivo ECMs; however, this is in a physiologically relevant concentration range and also maintains its structural stability, which is essential in mechanical testing.[27]

We developed a direct and reproducible method to cast the cross-linked PC12 collagen scaffolds. Molds were created to encapsulate the 3D NITC systems by mounting a circular acrylic ring (12 mm ID/15 mm OD) to a 25 mm coverslip using Norland 85 biocompatible glue to enable a clear path for imaging and housing of the PC12 collagen scaffolds (**Figure 1**B). After loading the cells into collagen on acrylic ringed coverslips, spinning disk confocal microscopy imaging was done to examine the NGF induced PC12 cells. The cells displayed a distinct green fluorescence signal with a 3:1000 dilution factor (2 mL F-12K Medium, 6 µL of diluted Fluo-4-AM dye) from the Fluo-4-AM loaded NGF induced PC12 cells (Figure 1C). Additional information on cell-culture, live-cell fluorescent imaging, and techniques to analyze a multi-dimensional ECM are in the Experimental Section and Supporting Information (Table S1).

2.2. Mechanical Excitation Testbed System

One promising approach for applying systematic mechanics is our mechanical excitation testbed (MET) that implements a voice coil actuator (VCA) to impose different modes of fast mechanical stimulation including single stimulation
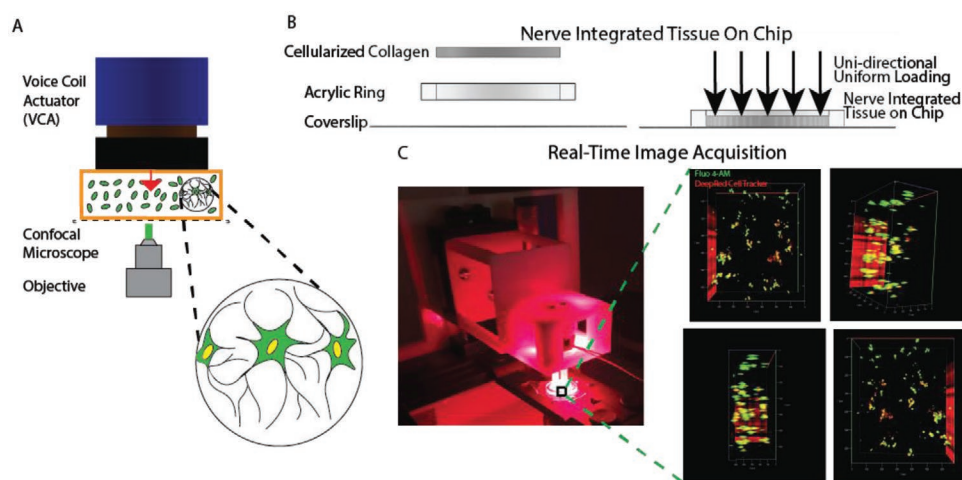

Figure 1. 3D in vitro neuron on a chip to probe mechanostimulation. A) The NITC approach in the MET system. B) Cellular collagen with PC-12 embedded in it is placed inside a custom acrylic housing ring, which is attached to a coverslip for imaging. The MET system applies a controlled downward force using a VCA. C) An image of the system for mechanically stimulating the NITC system with selected frames from a rotation of 3D reconstructed images (500 µm thickness: 0°, 45°, 90°, 180°) captured with confocal microscopy of NGF induced PC-12 cells dispersed through the collagen scaffold labeled with Fluo-4 AM and Deep Red Cell Tracker.
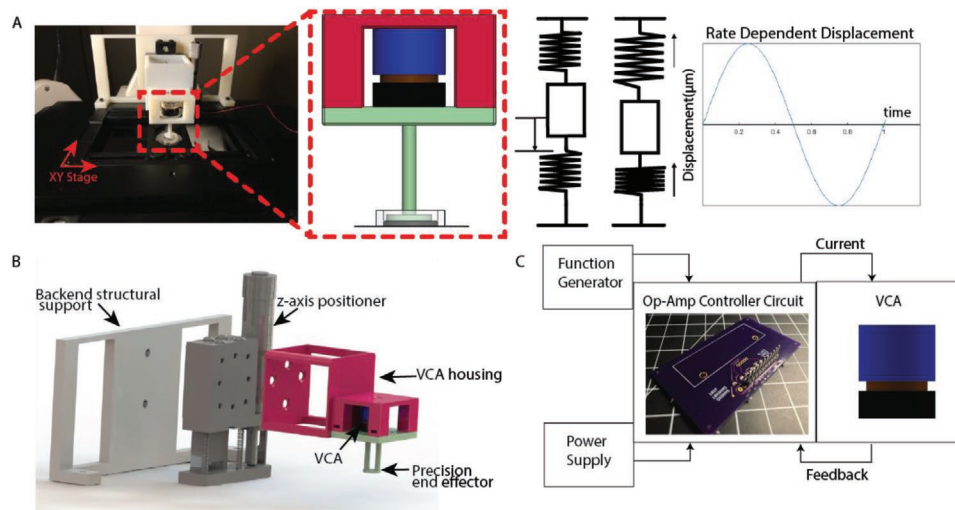
Figure 2. MET system for mechanical stimulation of PC-12 cells. A) Image of the MET system demonstrating the displacement over time functionality of the device. B) CAD drawing of the MET system consists of a custom 3D printed housing with a VCA assembly aligned with a spinning disk confocal microscope for real-time imaging. Mounting a z-axis positioner to a 3D printed structural support which is connected to a two-axis stage allows us to position the precision end effector component for mechanical stimulation of the collagen-cell NITC. C) A function generator that generates a sine waveform is created with a DC-coupled high gain custom electronic voltage amplifier circuit and a single-ended output to smooth the signal for actuating the VCA with the same waveform and frequency. The end effector actuates to apply compression and enable imaging of cells under mechanical stimulation.

excitation (s-stim) and repetitive stimulation (r-stim) excitation onto 3D collagen scaffolds. We designed our approach so that we apply mechanical stimuli that would mimic different degrees of important neuromechanics occurring in more physiologically relevant areas. One of these areas that we mimic is head injuries, as the degree of injury severity is distinguished as mild, moderate, or severe, and consists of primary and secondary phases.[28,29] The primary phase is the initial point of active mechanical stimulation while the secondary phase is the period post stimulation. During the primary phase, the force transduced is largely compressive from the initial impact-derived deformation.[30–33] With our approach using the MET system, we can apply controllable and tunable compression to our cellularized 3D biomaterial, collagen gels, to mimic degrees of injury severity under mechanical stimulation on our 3D models.

The MET system [**Figure 2**; Equations (S1)–(S4), Supporting Information] applies systematic uniaxial rectilinear compressive motion to the cellularized collagen gels by modulating a linear voice coil (VCA) (HVCM-016-010-003-01; Moticont, Van Nuys, CA) housed inside a custom (Solidworks Corp., 2018) 3D printed (Object350) housing with a precision force applicator arm (named "end effector"). The custom 3D printed stand is connected to a linear stage (4053 Parker Daedal Ball Bearing Positioner) used for precise positioning of the force applicator arm. The incorporation of a VCA allows for controllable and tunable actuation through the position interval displacement as a function of time. The VCA is powered and controlled using a function generator and a custom printed electronic circuit board (PCB) (EAGLE, AutoDesk) (Figure 2C; Figure S1, Supporting Information). To account for the inherent noise from the VCA, an operational amplifier (OPA544T) was designed into the PCB. The PCB board combined component placement and routing layouts to control electrical connectivity. Current flows from the op-amp PCB board to the VCA in a feedback loop.

The MET generates controlled displacement waveforms (Figure 2A) over a wide range of frequencies to simulate mild to severe external mechanical loading based on previous cellular TBI investigations, which applied strain rates that span 10^{-4} to 75 s^{-1}.[11,34] Tuning the frequency, amplitude, and waveform changes the dynamic movement of the VCA from lower strain rate quasistatic motion loading to high strain rate dynamic motion loading. The studies presented here are all conducted using a sine waveform and model repeated applied strains.

Gathering information in real time is important for understanding the response of cells during different phases of stimulation. One challenge with using tissue-on-a-chip systems with 3D in vitro gels is viewing changes such as movement of the system, which occurs with mechanical stimulation, using standard epifluorescence microscopy. Even more complicated is that 3D gels have cells in different planes and not just in a singular plane as is found in most 2D cell culture systems. To accommodate this, the MET device contains a structural support which mounts to the manual two axis stage directly in line with a spinning disk confocal microscope for controlled imaging. Combining the MET system with a high powered objective yields a working distance that can facilitate imaging of cells in different planes (Figure 1C). Our setup is also able to examine cells through the different z planes after the cellularized collagen gel is displaced by the precision end effector. Through capturing images during the entire mechanical stimulation, our approach is able to examine cells during each cycle as the cells return to the plane where the microscope is focused.
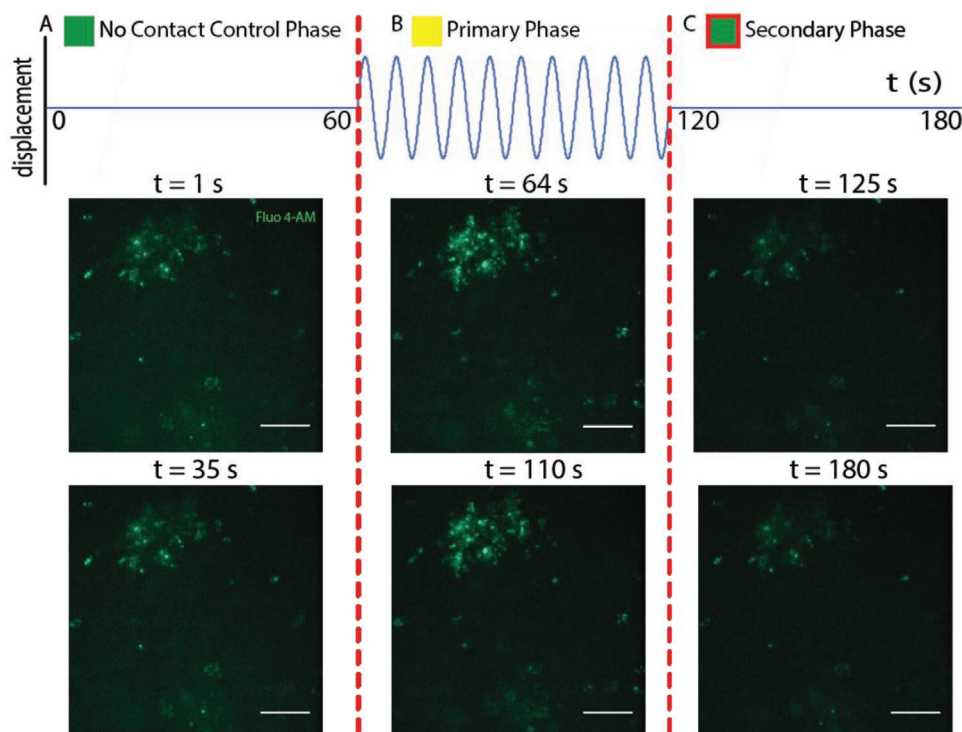
**ADVANCED
SCIENCE NEWS**
www.advancedsciencenews.com

**ADVANCED
BIOSYSTEMS**
www.adv-biosys.com

Figure 3. Ca^{2+} response during no-contact control phase, primary phase, and secondary phase mechanical stimulation in 3D NITC system. Representative schematics of displacement versus time for the mechanical stimulation. Images of the Fluo-4AM labeled differentiated PC-12 cells using spinning disk confocal fluorescent microscopy for A) no-contact control phase, (B) primary phase, and C) secondary phase. Red box indicates areas where cells in the focal plane with Ca^{2+} were analyzed at a strain rate of $\dot{E} = 4 \times 10^{-2}$ s^{-1}. Scale bars, 100 μm.

2.3. Analysis of Ca^{2+} Labeled Differentiated PC12 Cells during Mechanical Excitation

To study the in vitro Ca^{2+} response for differentiated PC12 cells in 3D collagen scaffolds when stimulated by MET, precise imaging of the response over time was essential (**Figure 3**). To capture images, a 1 Hz frequency for the VCA was used through the function generator while applying controlled systematic amplitudes of strains to the gels. This approach allowed the ability to select a focal plane with cells in focus and then to stimulate the cells while capturing images. The experimental testing included a 60 s no-contact control phase, 60 s r-stim sine wave primary phase, and a 60 s secondary phase while imaging the Ca^{2+} labeled differentiated PC12 cells in collagen scaffolds (**Figure 4**).

The fluorescence response of the differentiated PC12 cell gels changes over time for each strain rate as observed in the distinct changes beginning at the primary phase. The first change within the NITC system was the immediate increase in intensity of Ca^{2+} (Figures 3: Primary Phase, 4B,4C; Figures S2, S3, Movie S1, Supporting Information). Images during the no-contact control phase remained at a steady state over the entire 60 s span for all 6 samples and pixel intensity was measured as an absolute maximum of Ca^{2+} (Figures 4A,D). Through analyzing the effects over time on the spatiotemporal distributions of Ca^{2+}, strain rate appears to have a distinct effect on Ca^{2+} in the neurons (Figure 4). For the two impact loading rates (4 × 10^{-2} and 8 × 10^{-2} s^{-1}), the primary phase had a significant difference in both peak maximum intensity and peak mean

expression levels experienced by the 3D embedded cells (Figures 4D–G). We analyzed fluorescent cell response (Figures 4A–C), which showed distinct changes after mechanical loading. An immediate increase with external mechanical excitation occurred in all of the samples regardless of the applied strain rate in the primary phase (Figures 4B,E,G; Figures S2,S3, Supporting Information). The red and blue data points of the primary phase (Figure 4E) are the recorded relative maximum Ca^{2+} intensity during each frame of time corresponding to cells going in and out of focus (Figure S3, Supporting Information). For $E = 4 \times 10^{-2}$ s^{-1}, we observed a Ca^{2+} increase of 9.74% and 17.3% for $E = 8 \times 10^{-2}$ s^{-1}(Figure 4G) which can be visually shown in the images of each phase (Figures 4A–C). The distribution of pixel intensity as a relation to strain rate is greater during the primary phase resulting in a higher mean Ca^{2+} intensity (Figure 4G). The mechanically induced elevation in Ca^{2+} was not sustained following the primary phase and immediately began to decline in all tests (Figure 4G). During the secondary phase, the maximum Ca^{2+} intensity signal fluctuated during the 60 s window. This finding might be particularly important as altered Ca^{2+} homeostasis is linked to several neurodegenerative diseases including TBI.[34–36] Our work has findings that align with others in the literature from a mechanics and Ca^{2+} perspective such as biomechanics and tissue deformations[11,37–40] along with cellular Ca^{2+} levels.[41–48] These previous papers show that after stretch and shear, cellular Ca^{2+} level exhibits comparable dynamic shifts to our reported work from 3D compressive loading. Rzigalinsk, et al. reported following

**ADVANCED
SCIENCE NEWS**
www.advancedsciencenews.com
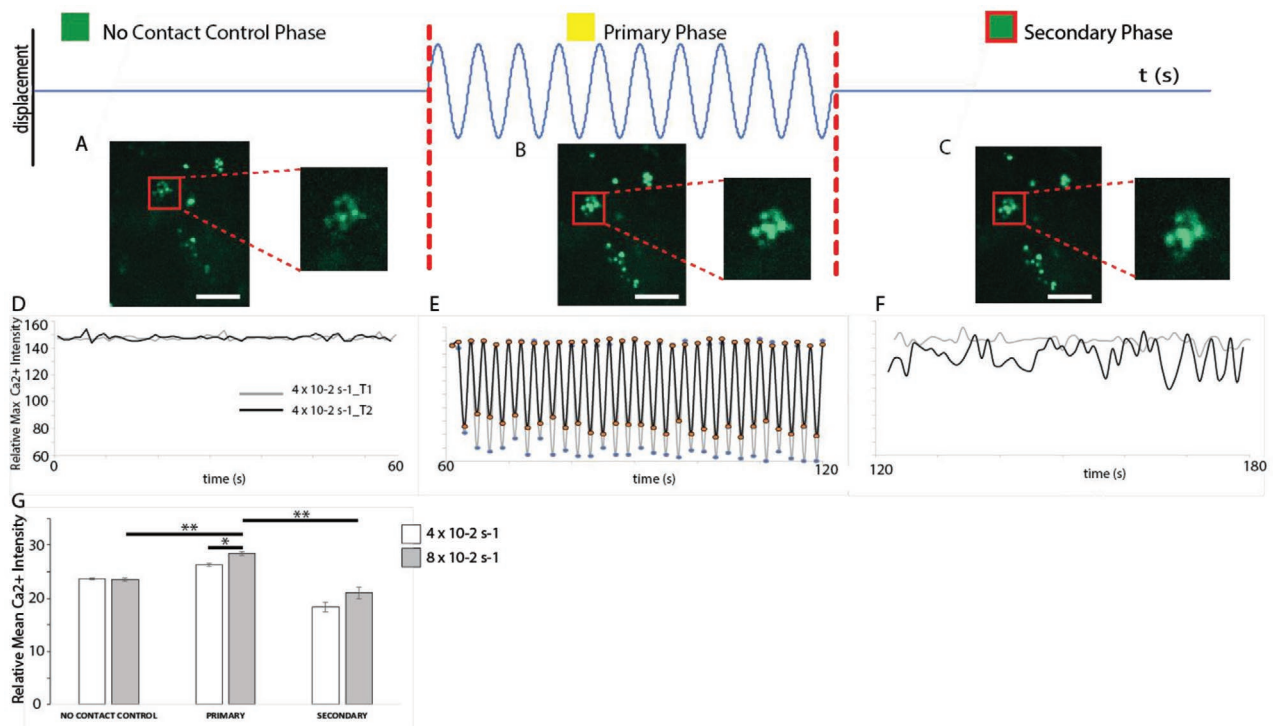
**ADVANCED
BIOSYSTEMS**
www.adv-biosys.com

Figure 4. Analysis of Ca^{2+} under mechanical stimulation for the NITC system. Frames from $\dot{E} = 4 \times 10^{-2}$ s^{-1} sample with A) no-contact control phase, B) primary phase, C) secondary phase. Scale bars, 50 µm. D) Quantification of the same strain rate, $\dot{E} = 4 \times 10^{-2}$ s^{-1} at 1 Hz frequency, cell response denoting the no-contact control phase maximum Ca^{2+} intensity values. (T1 and T2 are different representative experiments). E) Panel denotes maximum Ca^{2+} intensity during the primary phase. F) Panel denotes the secondary phase of maximum Ca^{2+} intensity. G) Bar graph plot comparing the mean Ca^{2+} ion intensity before, during, and after the primary phase at strain rates of $\dot{E} = 4 \times 10^{-2}$ s^{-1} (white bar) and 8×10^{-2} s^{-1} (gray bar). Data presented as mean ± SD, $n = 6$, p-values are calculated using t-test, *$p \leq 0.05$, **$p \leq 0.01$.

stretch injury, Ca^{2+} is rapidly elevated proportional to the degree of injury.[45] In the studies, Ca^{2+} elevation was not sustained after the stretch injury and returned to near-basal levels post injury. Maneshi et al. reported that following shear stress increased Ca^{2+} depended on the magnitude, duration, and rise time of the stimulus,[46] which is aligned with our findings.

3. Conclusion

This study presents a 3D tissue-on-a-chip neural system which examined cell response under mechanical stimulation. We designed a mimetic in vitro ECM collagen scaffold embedded with NGF induced PC12 cells and applied our MET system to assess spatiotemporal molecular response to external compressive stimulation. The creation of the MET device allowed us the flexibility for stimulation of the 3D tissue-on-a-chip system by enabling systematic mechanical stimulation with live confocal imaging. With the ability to image the microenvironment under mechanical stimulation, new spatiotemporal details of in vitro Ca^{2+} responses during the no-contact control phase, primary phase, and secondary phase were found relative to strain rate. Given the frequency and prevalence of compressive loading during external mechanical impacts in different systems including to the head, the 3D in vitro findings of this study provide insight into the cell response relative to mechanical loading in an important area of Ca^{2+} signaling. This

work could be a foundational building block to merging 3D in vitro multi-dimensional ECMs with architecture, bioactive, and mechanical cues to advance neuropathomorphology assessment. Future studies could also address variation of strain rates used to elicit biosensor response, ECM complexity, as well as machine learning based approaches to examine injury through in vitro based approaches.

4. Experimental Section

Cell Culture: PC12 cells (ATCC, CRL-1721) were cultured in F-12K Medium (Kaighn's Modification of Ham's F-12 Medium) (ATCC 30–2004) supplemented with 5% fetal bovine serum and 10% horse serum. Cells were maintained in a humidified incubator held constant at 37 °C with ≈5% CO$_2$. The collagen IV solution was prepared by mixing 5 mg of collagen IV and 5 mL of 0.25% acetic acid for 2 h and coating the device overnight at 4 °C. Cells were plated in the collagen IV coated devices and allowed to grow to confluency following standard subculture protocol.[49]

Fluorescent Ca^{2+} Labeling and Imaging with Live Cell Capture: Fluo-4-AM (stock: 50 µg, molecular weight: 1097 g mol^{-1}), which is a cell permeant Ca^{2+} indicator, was diluted with DMSO as described by the ThermoFisher Scientific protocols. For 3D in vitro cellularized collagen scaffolds, 3:1000 dilution factor (2 mL F-12K Medium, 6 µm of diluted Fluo-4-AM dye) was used for Ca^{2+} labeling.[50] PC12 cells with 50 ng mL^{-1} of NGF were incubated for 1 h with Fluo-4-AM. Prior to Ca^{2+} imaging, Ca^{2+} stained cells were added to 10X PBS, NaOH, and type 1 collagen to form the cellularized ECM. The ECM was then allowed to cross-link

**ADVANCED
SCIENCE NEWS**

www.advancedsciencenews.com

**ADVANCED
BIOSYSTEMS**

www.adv-biosys.com

for 1 h before imaging. During mechanical stimulation, a spinning disk confocal microscope captured images at controlled speeds.

NITC Device: To create an integrated 3D cellularized model tissue as an in vitro testing platform with mechanics, a biomaterials approach was combined with a mechanical testing approach (Figure 1). NITC devices were constructed with collagen 1 and 50 ng mL^{-1} NGF induced PC12 (ATCC, CRL-1721) cells to promote neurite outgrowth. NGF induced PC12 cells were cultured in F-12K Medium (Kaighn's Modification of Ham's F-12 Medium) (ATCC 30–2004) supplemented with 5% fetal bovine serum and 10% horse serum on collagen IV coated flasks. Cells were maintained in an incubator held constant at 37 °C with ≈5% CO_2 with a medium change every 48 h. Cells were allowed to grow to 80–90% confluency to an observable change in sympathetic neuron phenotype.

NITC Device Imaging: 3D NITC devices were plated on 25 mm coverslips surrounded by an acrylic ring chamber. The NITC device assembly was mounted on the stage of an inverted, spinning disk confocal microscope (Axio Observer Z1 Microscope System, Zeiss) with both a function generator (Agilent 33120A Function Generator) and a power supply (BK Precision 1760A Triple Output Power Supply). An oscilloscope (Rigol 100 MHz Digital) was also incorporated to verify the waveform of the signal with one for the signal of the function generator and another for the signal from the VCA. A custom printed circuit board using a high current, high voltage operational amplifier (OPA544T, Texas Instruments) was used to decrease the noise; the operational amplifier smoothed the signal from the VCA. Image capture was synchronized with the MET at a frequency of 1 Hz resulting in 180 images which were post-processed using python and NIH ImageJ software.

Statistical Analysis: Continuous variables are expressed as mean ± SD. For all datasets, t-tests were conducted across all groups with significance defined as $*p \leq 0.05$ and $**p \leq 0.01$. Statistical analysis was through NIH ImageJ and Microsoft Excel.

Supporting Information

Supporting Information is available from the Wiley Online Library or from the author.

Conflict of Interest

The authors declare no conflict of interest.

[1] I. Wagner, E. M. Materne, S. Brincker, U. Süßbier, C. Frädrich, M. Busek, F. Sonntag, D. A. Sakharov, E. V. Trushkin, A. G. Tonevitsky, R. Lauster, *Lab Chip* **2013**, *13*, 3538.

[2] L. G. Griffith, M. A. Swartz, *Nat. Rev. Mol. Cell Biol.* **2006**, *7*, 211.

[3] L. Wan, J. Skoko, J. Yu, O. B. Ozdoganlar, P. R. LeDuc, C. A. Neumann, *Sci. Rep.* **2017**, *7*, 16724.

[4] L. Wan, P. R. LeDuc, C. Neumann, *FASEB J.* **2017**, *31*, 942.

[5] I. Ferrer, R. Blanco, M. Carmona, B. Puig, M. Barrachina, C. Gomez, S. Ambrosio, *J. Neural Transm.* **2001**, *108*, 1383.

[6] C. Li, Y. Hu, M. Mayr, Q. Xu, *J. Biol. Chem.* **1999**, *274*, 25273.

[7] Y. Wang, E. L. Botvinick, Y. Zhao, M. W. Berns, S. Usami, R. Y. Tsien, S. Chien, *Nature* **2005**, *434*, 1040.

[8] Y. W. Lin, C. M. Cheng, P. R. LeDuc, C. C. Chen, *PLoS One* **2009**, *4*, e4293.

[9] D. Zhang, M. Pekkanen-Mattila, M. Shahsavani, A. Falk, A. I. Teixeira, A. Herland, *Biomaterials* **2014**, *35*, 1420.

[10] S. H. Choi, Y. H. Kim, M. Hebisch, C. Sliwinski, S. Lee, C. D'Avanzo, H. Chen, B. Hooli, C. Asselin, J. Muffat, J. B. Klee, *Nature* **2014**, *515*, 274.

[11] E. Bar-Kochba, M. T. Scimone, J. B. Estrada, C. Franck, *Sci. Rep.* **2016**, *6*, 30550.

[12] Centers for Disease Control, Prevention, www.cdc.gov/traumatic-braininjury/pubs/tbi_report_to_congress.html. (accessed: January **2016**).

[13] M. C. Dewan, A. Rattani, S. Gupta, R. E. Baticulon, Y.- C. Hung, M. Punchak, A. Agrawal, A. O. Adeleye, M. G. Shrime, A. M. Rubiano, J. V. Rosenfeld, K. B. Park, *J. Neurosurg.* **2018**, *130*, 1080.

[14] G. J. Augustine, F. Santamaria, K. Tanaka, *Neuron* **2003**, *40*, 331.

[15] E. M. Brown, R. J. MacLeod, *Physiol. Rev.* **2001**, *81*, 239.

[16] D. E. Clapham, *Cell* **2007**, *131*, 1047.

[17] M. P. Mattson, F. M. LaFerla, S. L. Chan, M. A. Leissring, P. N. Shepel, J. D. Geiger, *Trends Neurosci.* **2000**, *23*, 222.

[18] P. R. Heath, P. J. Shaw, *Muscle Nerve* **2002**, *26*, 438.

[19] T. Nakamura, S. A. Lipton, *Cell Calcium* **2010**, *47*, 190.

[20] U. Wojda, E. Salinska, J. Kuznicki, *IUBMB Life* **2008**, *60*, 575.

[21] D. J. Surmeier, J. N. Guzman, J. Sanchez-Padilla, *Cell Calcium* **2010**, *47*, 175.

[22] T. A. Lusardi, J. A. Wolf, M. E. Putt, D. H. Smith, D. F. Meaney, *J. Neurotrauma* **2004**, *21*, 61.

[23] Y. J. Yang, H. J. Lee, D. H. Choi, H. S. Huang, S. C. Lim, M. K. Lee, *Neurosci. Lett.* **2008**, *440*, 14.

[24] C. Morabito, S. Guarnieri, G. Fanò, M. A. Mariggiò, *Cell. Physiol. Biochem.* **2010**, *26*, 947.

[25] V. L. Cross, Y. Zheng, N. W. Choi, S. S. Verbridge, B. A. Sutermaster, L. J. Bonassar, C. Fischbach, A. D. Stroock, *Biomaterials* **2010**, *31*, 8596.

[26] C. B. Raub, A. J. Putnam, B. J. Tromberg, S. C. George, *Acta Biomater.* **2010**, *6*, 4657.

[27] V. V. Artym, K. Matsumoto, *Curr. Protoc. Cell Biol.* **2010**, *48*, 10.18.1.

[28] M. Brasure, G. J. Lamberty, N. A. Sayer, N. W. Nelson, R. MacDonald, J. Ouellette, J. Tacklind, M. Grove, I. R. Rutks, M. E. Butler, R. L. Kane, T. J. Wilt, *Multidisciplinary Postacute Rehabilitation for Moderate to Severe Traumatic Brain Injury in Adults*, AHRQ Publication, Rockville, MD **2012**.

[29] P. Kaur, S. Sharma, *Curr. Neuropharmacol.* **2018**, *16*, 1224.

[30] A. M. Nahum, R. Smith, C. C. Ward, SAE Technical Paper 770922, **1977**.

[31] R. H. Kraft, P. J. Mckee, A. M. Dagro, S. T. Grafton, *PLoS Comput. Biol.* **2012**, *8*, e1002619.

[32] R. M. Wright, K. T. Ramesh, *Biomech. Model. Mechanobiol* **2012**, *11*, 245.

[33] L. Young, G. T. Rule, R. T. Bocchieri, T. J. Walilko, J. M. Burns, G. Ling, *Front. Neurol.* **2015**, *6*, 89.

[34] J. T. Weber, *Front. Pharmacol.* **2012**, *3*, 60.

[35] T. Kristián, B. K. Siesjö, *Stroke* **1998**, *29*, 705.

[36] J. T. Weber, B. A. Rzigalinski, E. F. Ellis, *J. Biol. Chem.* **2001**, *276*, 1800.

[37] B. J. Pfister, T. P. Weihs, M. Betenbaugh, G. Bao, *Ann. Biomed. Eng.* **2003**, *31*, 589.

[38] H. Ahmadzadeh, D. H. Smith, V. B. Shenoy, *Biophys. J.* **2014**, *106*, 1123.

[39] D. K. Cullen, M. C. Lessing, M. C. LaPlaca, *Ann. Biomed. Eng.* **2007**, *35*, 835.

[40] E. F. Ellis, J. S. McKinney, K. A. Willoughby, S. Liang, J. T. Povlishock, *J. Neurotrauma* **1995**, *12*, 325.

[41] T. A. Lusardi, J. Rangan, D. Sun, D. H. Smith, D. F. Meaney, *Ann. Biomed. Eng.* **2004**, *32*, 1546.

[42] R. S. Cargill, L. E. Thibault, *J. Neurotrauma* **1996**, *13*, 395.

[43] M. C. LaPlaca, L. E. Thibault, *Ann. Biomed. Eng.* **1997**, *25*, 665.

[44] T. A. Lusardi, J. A. Wolf, M. E. Putt, D. H. Smith, D. F. Meaney, *J. Neurotrauma* **2004**, *21*, 61.

[45] B. A. Rzigalinski, J. T. Weber, K. A. Willoughby, E. F. Ellis, *J. Neurochem.* **1998**, *70*, 2377.

[46] M. M. Maneshi, F. Sachs, S. Z. Hua, *J. Neurotrauma* **2015**, *32*, 1020.

[47] Y. Cho, D. A. Porto, H. Hwang, L. J. Grundy, W. R. Schafer, H. Lu, *Lab Chip* **2017**, *17*, 2609.

[48] L. Liu, H. Li, Y. Cui, R. Li, F. Meng, Z. Ye, X. Zhang, *Cell. Physiol. Biochem.* **2017**, *42*, 441.

[49] D. J. Shiwarski, M. Darr, C. A. Telmer, M. P. Bruchez, M. A. Puthenveedu, *Mol. Biol. Cell* **2017**, *28*, 2202.

[50] ThermoFisher Scientific, https://www.thermofisher.com/document-connect/document-connect.html?url=https%3A%2F%2Fassets.thermofisher.com%2FTFS-Assets%2FLSG%2Fmanuals%2Fmp01240.pdf&title=Rmx1byBDYWxjaXVtIEluZGljYXRvcnM=[Accessed 25 Sep. 2019] (accessed: September **2011**).